ELSEVIER

Journal of Molecular Structure 405 (1997) 29–44

Journal of
MOLECULAR
STRUCTURE

Applications of surface enhanced Raman scattering to the study of metal–adsorbate interactions

Alexandre G. Brolo, Donald E. Irish*, Brian D. Smith

Guelph-Waterloo Centre for Graduate Work in Chemistry, Department of Chemistry, University of Waterloo, Waterloo, Ont. N2L 3G1, Canada

Abstract

Surface enhanced Raman scattering (SERS) is a powerful technique for characterizing adsorbed species and processes at metallic surfaces. The giant signal enhancement (10^4–10^6 larger than normal Raman scattering) makes this technique sensitive to even sub-monolayer amounts of adsorbate on a surface. Consequently, the application of SERS to the in situ study of electrochemical processes provides useful mechanistic and structural information. In this review, advantages and limitations of electrochemical SERS techniques are presented along with experimental information about the nature of the metal–adsorbate interactions occurring in various aqueous and non-aqueous systems. Special emphasis is given to experimental results; however, the salient features of the enhancement theories are highlighted. Adsorbate orientation and SERS surface selection rules are discussed.

Keywords: Surface enhanced Raman scattering; Metal adsorbates

1. Introduction

Surface enhanced Raman scattering (SERS) was first recognized about 20 years ago [1,2]. At that time, investigators anticipated that in situ studies of the electrochemical interphase would be revolutionized by the giant enhancement of the Raman scattering. Unfortunately, the necessity of creating a rough surface and the small number of metals (mainly, Au, Ag, and Cu) [3] supporting the effect in the visible region are factors that seriously limit the application of this technique in electrochemistry. However, even with these restrictions, the electrochemical SERS technique has been widely used for the study of metal–adsorbate interactions. Its applications range from "classical" electrochemical studies such as corrosion processes [4,5], film growth [6], and self-assembled monolayers [7] to medical applications [8] and trace analysis [9,10]. These applications suggest that electrochemical SERS is a well established field with potential for advancement; however, the earlier controversy about the nature of the enhancement mechanism can confuse a non-SERS specialist wanting to apply the technique to a specific problem of electrochemical, analytical, or biological interest. Several reviews [11–16] have helped to disseminate the basic principles of the technique and broaden its range of applications. Some of these reviews are very comprehensive [17,18], and others emphasize specific applications, for instance to

* Corresponding author.

0022-2860/97/$17.00
PII S0022-2860(96)09426-4

biological [19] and to analytical problems [20]. Here, the important features of electrochemical SERS will be presented. The most important contributions to the overall enhancement, and the expected dependence of the SER intensities on applied potential, excitation wavelength, surface coverage, and surface morphology inferred from these theories will be discussed. Finally, the limitations and pitfalls will also be presented.

2. Experimental

2.1. Cell design

In order to observe SERS, it is necessary to design and construct a cell which combines good electrochemical and spectroscopic performance. Often the design criteria must be constrained by the nature and location of the collection and focusing optics of the spectrometer. We have designed an electrochemical cell (Fig. 1) which can be used in a conventional Raman arrangement where the focusing and collection optics are parallel to the floor (the *XY* plane) and at 90° to each other. Cells are readily interchangeable and thus allow several experiments to be carried out with a minimum of realignment work. A standardized cell can be mounted on a stage consisting of an *XY* translation stage (Optikon) and a rotation stage to allow full rotation in the *XY* plane (Kinetic Systems). A tilt stage is also provided (Kinetic Systems) along with a vertical adjustment (*Z* translation) stage (in-house). Thus, the angle of incidence between the electrode and laser beam can be accurately and reproduceably set.

The cell body is a 25 mm threaded Ace Glass fitting. Two 7 mm Ace Glass connectors were glass-blown to the sides to accomodate the Luggin capillary and the counter electrode compartments. A 19/26 ground glass joint was fused to the top of the cell to allow the attachment of a bubbler for purging the cell. The components can easily be attached and disassembled via the threaded Teflon fittings and ferrules. The cell window is attached via a specially designed plate which allows a tight seal. The seal is achieved with a thin Teflon washer and a rubber O-ring seal on either side of the optical window, ensuring that the glass is not broken by the pressure applied

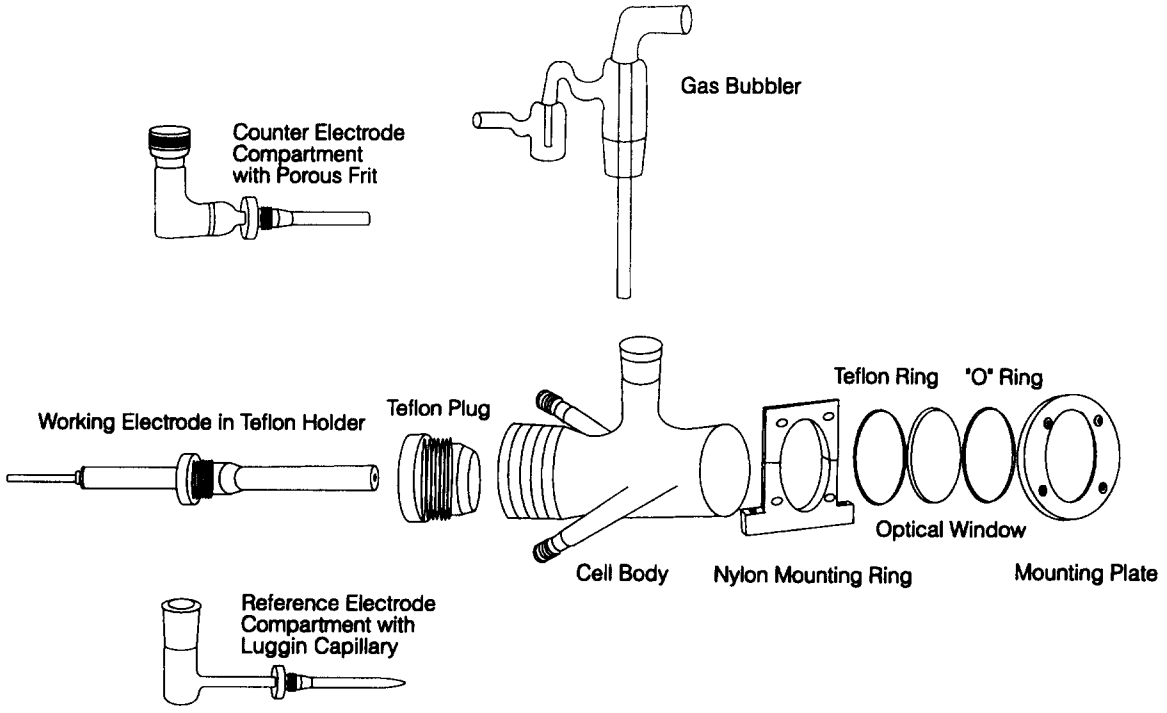

Fig. 1. The spectroelectrochemical cell and the working electrode.

through the screws and the solution is only in contact with the Teflon seal. This overcomes two concerns: windows that are attached by glass-blowing techniques tend to distort; windows attached by epoxy adhesive risk introduction of contaminants.

The counter electrode is isolated from the main solution by a porous frit and the reference electrode is connected via a Luggin capillary tube. The working electrode and Teflon holder are machined so that the electrode can be slid snugly in and out of the Teflon. Although this arrangement will not completely prevent leakage of the solution around the sides of the electrode it does allow the electrode to be removed for cleaning (electrodes set into Teflon by heating still have gaps between the electrode and holder which can trap solution and are impossible to clean). A brass rod is screwed into the back of the electrode, in order to provide electrical contact. The portion of the brass rod inside the holder, which is not connected inside the electrode, is covered in Teflon tape to help prevent reaction with any solution that might migrate past the side of the electrode. The electrode is then threaded in the back of a 25 mm Teflon plug and mounted in the cell.

2.2. Electrode preparation

The electrode preparation, consisting of polishing, cleaning and finally roughening by the application of one or more oxidation–reduction cycles (ORCs), is designed to remove metal from the electrode surface and redeposit it as small-scale SERS-active surface roughness. The ORC can be accomplished by either a potential step or a potential sweep. The specific ORC conditions, such as the anodic and cathodic limits, the potential step hold time or the potential sweep speed will tend to vary from system to system and some experimentation is usually required in order to achieve the optimum SERS scattering.

Silver is the most commonly employed working electrode because its SERS response is activated by the 514.5 nm line of an argon ion laser. A SERS-active silver electrode can be prepared by mechanically polishing the electrode with alumina (progressively finer grades, finishing with 0.3 μm) and roughening the electrode in a halide medium. A factor for silver is the interaction of the surface species formed during the ORC with the laser light. Silver salts are photosensitive and illumination of the electrode during the ORC gives an increase in the SERS intensity [21]. The light aids the deposition of small-scale roughness by photochemically depositing more metal onto the surface. It has been reported, however, that this can lead to some irreproducibility in the observed SERS [14].

Copper electrodes can be prepared by mechanical polishing with ultra-fine sand paper and 0.3 μm alumina, followed by electrochemical or chemical polishing. Copper provides an interesting example of how the nature of the system can determine the requirements of the ORC. It has been found, for example, that the SERS of pyridine on copper electrodes in 0.1 M KCl solution can be observed at open circuit potential without an ORC owing to the creation of SERS-active roughness by a corrosion process [22]. The SERS of pyridine adsorbed onto copper is also observable even at very negative potentials.

It is possible to prepare a very stable SERS-active surface on gold electrodes. The electrode is mechanically polished with 1.0 and 0.3 μm alumina, and roughened in chloride solution. The gold electrode can be roughened ex situ, washed and used in another solution with good results. The quality of the SERS signal is dependent on the number of ORCs performed [23].

2.3. Experimental set-up

The electrochemical status of an experiment is readily monitored by observing the voltammograms produced during the ORCs; these provide an overall view of the performance of the system. Calibration of the spectrometer is easily accomplished using a reference spectrum such as a neon lamp.

Birke et al. [14] provide a comprehensive list of parameters that are important in SERS experiments. Two of these are the polarization of the incident light and the angle of incidence. For smooth surfaces, p-polarized light must be employed in order to observe surface species [24]. For rough surfaces, we have found that either s- or p-polarized light can provide good quality SERS spectra. The incident polarization can often be chosen in order to increase or reduce the intensity of scattering from solution species. It has been noted that the optimal angle of incidence for

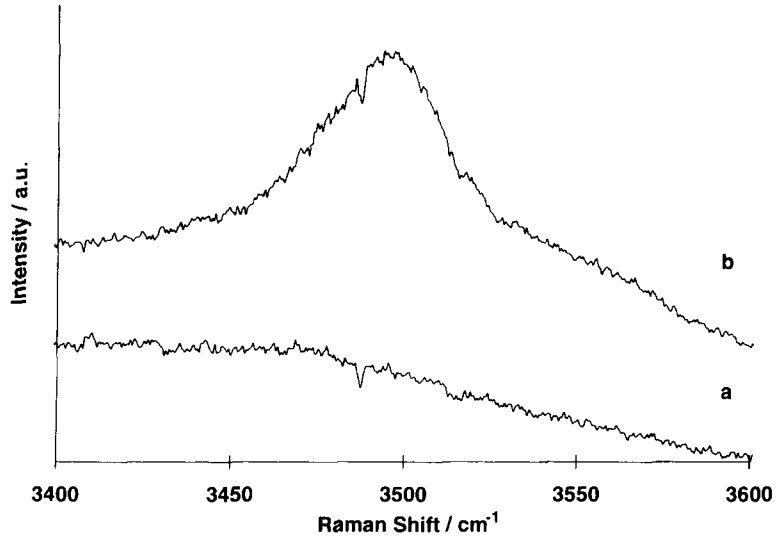

Fig. 2. Spectrum from a Ag electrode in 1.0 M KBr: (a) before the ORC; (b) after the ORC (from − 700 to − 50 mV at 5 mV s^{-1} under laser illumination). The signal from adsorbed water can be observed at about 3510 cm^{-1} (E = − 400 mV).

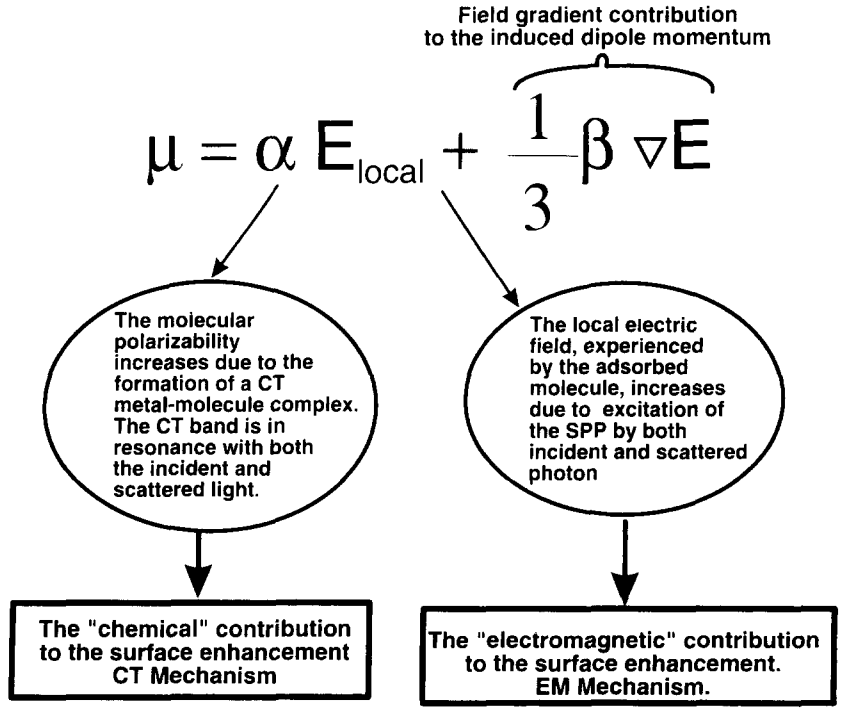

Fig. 3. The induced molecular dipole (μ) for a molecule adsorbed onto a metallic surface. α is the molecular polarizability, E_{local} is the electric field experienced by the molecule, β is the quadrupole polarizability and ∇E is the electric field gradient. The vector and tensor representations were omitted for simplification.

SERS is about 62° [25] but, for a heavily roughened surface, this need not be closely adhered to; however, for moderately and lightly roughened surfaces, this angle is important.

It is advantageous to have a SERS reference system which ensures that alignment is optimized. One of the best systems we have found for routine alignment purposes is 1 M KBr with silver [26]. If a single ORC is run from − 0.7 to − 0.05 V (vs. SCE) with a sweep rate of 5 mV s^{-1}, under laser illumination, the 3510 cm^{-1} SERS stretching band of adsorbed water appears at about − 0.4 V on the cathodic sweep cycle (Fig. 2). This system is useful for alignment for several reasons: it is easy to set up, the SERS signal is consistently observable, and the SERS signal is not as intense as for other systems (e.g. pyridine). As a result, it is possible to use this system to provide a check that the alignment of the cell is correct. If the signal from the relatively weak band of water at about 3500 cm^{-1} is maximized, good alignment is assured. The alignment can also be readily checked by observing the weaker water bending mode band at 1615 cm^{-1}.

3. Why does the enhancement occur?

The intensities of the inelastic scattered light in a normal Raman spectroscopy (NRS) experiment are proportional to the square of the induced dipole moment (μ). For a molecule adsorbed onto a metallic electrode surface, and therefore subjected to an additional electric field from that surface, the induced dipole moment is given by the expression in Fig. 3. An additional field gradient term is included owing to the inhomogeneous electric field enveloping the molecule. The two most important mechanisms that contribute to the overall enhancement are related to an exceptional increase in both the molecular polarizability (α) of the adsorbed species and the local electric field (E_{local}) near the metallic surface. The former accounts for the "chemical" or "charge transfer (CT)" mechanism and the latter for the "electromagnetic (EM)" mechanism. There has been a dispute as to which of these mechanisms is dominant. Most authors now agree that both mechanisms contribute to the overall effect; however, one or other of them can be dominant for certain systems. Some of the important aspects of both mechanisms will be presented in the next sections; a detailed description of the CT [27,28] and EM mechanisms [29] can be found elsewhere, and a general discussion involving quantum mechanical aspects of the enhancement has appeared in a review by Pettinger [18].

3.1. The electromagnetic contribution to SERS — the EM mechanism

In the EM mechanism, the enhancement of the Raman signal occurs as a result of coupling between the incident light and the electron oscillations at the metallic surface, known as surface plasmons (SPs). The SPs are confined to a smooth surface and cannot be excited by the incident photon owing to a momentum mismatch [18]. The bumps in a rough surface provide additional momentum for the photon, and the SPs can be excited. For surface features smaller than the optical wavelength, the SP normal modes of oscillation can be resonant with both the exciting and the scattered photons. This coupling concentrates the electromagnetic field in certain regions of the surface. The frequency of the SP oscillations depends on the dielectric constant of the metal, which accounts for the observation of SERS signals from only a few metals (Cu, Ag, Au, alkali metals) [3,30]. The EM enhancement depends only on the characteristics of the metal; hence, vibrational modes with the same symmetry species should have the same enhancement factor for the same surface morphology.

3.2. The "chemical" contribution to SERS — the CT mechanism

Some experimental results suggest that another mechanism also plays a role in the overall enhancement. For instance, the fact that different molecules with similar polarizability, adsorbed onto the same metallic substrate, exhibit distinctly different enhancement factors cannot be explained by only EM arguments [27,28]. In this additional "chemical" mechanism, the enhancement is due to a CT complex formed between the atomic scale roughness on the metal (adatoms) and the adsorbed molecule. The energy of the frontier molecular orbitals of the adsorbed molecule is close to the metal's Fermi level because of the complex formation. The difference in

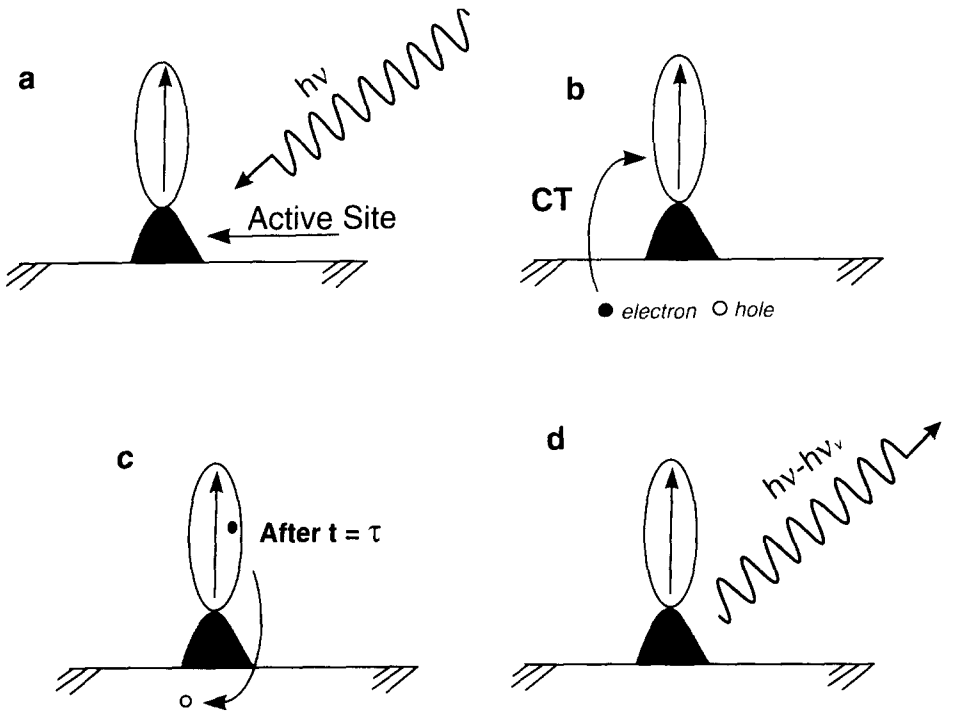

Fig. 4. The photon-driven charge transfer mechanism (PDCT). (a) The radiation bathes a molecule adsorbed onto an atomic scale active site. The interaction leads to the formation of an electron-hole pair. This process occurs at an enhanced rate on these adatom sites. (b) The electron tunnels from the metal to the molecule. (c) If the electron resides in the molecule long enough for a vibrational change (τ), it will carry this information when it tunnels back to the metal. (d) The annihilation of the electron occurs by recombination with the hole, and a Raman photon is created.

energy between the Fermi level and the frontier orbital of the adsorbed species is close in frequency to the incident light, and an enhancement mechanism occurs, which is analogous to the resonance Raman process [31]. A CT process can also occur via an increase in the metal's electron–photon coupling in the atomic scale roughness, which leads to a large production of electron-hole pairs. This process is described in Fig. 4, and is known as a photon-driven charge transfer (PDCT) mechanism.

A comparison of the main features anticipated by both models is presented in Table 1.

3.3. The SERS selection rules

SERS selection rules can be inferred from both CT and EM mechanisms [32].

For a situation where only the EM mechanism is important, a set of SERS selection rules can be exactly derived. The expression for the effective polarizability when an enhanced local electric field of a rough surface bathes the adsorbed molecule is given in Ref. [32]:

$$\alpha_{\text{eff}} = \frac{(\chi+1)^2}{(\epsilon_i+\chi)(\epsilon_s+\chi)} \begin{bmatrix} \alpha_{XX} & \alpha_{XY} & \kappa_s\alpha_{XZ} \\ \alpha_{YX} & \alpha_{YY} & \kappa_s\alpha_{YZ} \\ \kappa_i\alpha_{ZX} & \kappa_i\alpha_{ZY} & \kappa_i\kappa_s\alpha_{ZZ} \end{bmatrix} \quad (1)$$

Here, the subscripts i and s stand for incident and scattered radiation. The term χ corresponds to the polarizability of the metal aggregate of the rough surface, κ is related to the metal's dielectric constant, and Z is the axis perpendicular to the electrode surface.

The frequency of the incident photon is generally close to the frequency of the scattered light; hence, as a good approximation, one can consider that $\kappa_i \approx \kappa_s \approx \kappa$. Assuming that the direction of the vibration determines the contribution from the molecular polarizability tensor, an enhancement given by the relation $1 : |\kappa|^2 : |\kappa|^4$ is expected for modes transforming as

Table 1
Comparision of the salient features of the two most accepted surface enhancement theories

		CT mechanism	EM mechanism
1.	Origin	Resonance process involving the incident light and the CT band of the metal–molecule complex. (Resonance Raman-like process)	Enhancement of the local electric field due to the coupling of the incident photon with the metal's surface plasmons
2.	Roughness	Atomic scale roughness (active sites)	Large scale roughness (about 10–200 nm)
3.	Distance dependence	Short range. Important only for species adsorbed directly onto the surface	Long range. Important even for species several nm away from the surface, but decays with distance
4.	Potential dependence	The CT band can be tuned by the applied potential; therefore, the enhancement factor is potential dependent	The enhancement factor does not depend on the applied potential; intensity changes in the potential profile are due to the variation of the surface coverage with potential
5.	Excitation wavelength dependence	The resonance condition depends on the excitation wavelength. The potential at which the SER intensity maximizes (E_{max}) is different for different incident photon energies	The enhancement factor depends on the metal dielectric constant, which is wavelength dependent. E_{max} does not shift for different incident photon energies

α_{XY}, α_{YZ}, and α_{ZZ}, respectively. In other words, the modes with polarizability changes perpendicular to the surface must dominate the SERS spectrum.

The SERS selection rules can be used to determinate the orientation of molecules adsorbed onto the metallic surface. However, one must be aware that an additional contribution from the CT mechanism needs to be considered [33]. The CT process would enhance the symmetrical modes in general, and preferentially the modes involving the vibrational

Table 2
Summary of systems studied at the University of Waterloo

Electrode	Solvent	Adsorbed species	Comment	Reference
Ag	H_2O	Py, PyH^+, Cl^-	Ion pairs and neutrals	[72], [39]
Ag	H_2O	EDTA, Cl^-	Decomposition	[73]
Ag	CH_3CN	SCN^-	S bonding	[74]
Cu	H_2O	CuI, Cu_2O (?)	Surface films	[75]
Ag	CH_3CN	I^-, $[Li(CH_3CN)_x]^+$, $[Na(CH_3CN)_x]^+$, CH_3CN, H_2O, OH^-, OD^-, CN^-	Cation adsorption; H_2O reduction; decomposition	[76]
Ag	H_2O	DABCO, Cl^-	PDCT mechanism	[77], [44]
Ag	$CH_3CHCH_2CO_3$ (pc)	CO_3^{2-}, Br^-, I^-, H_2O, OH^-, pc	Decomposition	[78]
Au	H_2O	Py	Link to surface coverage	[55], [79]
Ag	H_2O	$DABCOH_2^{2+}$, Cl^-	pH dependence. EM mechanism	[40]
Au	H_2O	$Fe(CN)_6^{3-}$, $Fe(CN)_6^{4-}$	Depth profiling	[80]
Ag	H_2O	$DABCOH_2^{2+}/I^-$	Crystal growth. Depth profiling	[81], [82]
Ag	$CH_3CO_2CH_3$ (MA), HCO_2CH_3 (MF)	$[Li(MA)_4]^+$, $(CH_3)_4N^+$, Br^-	Ion pairs	[41], [58], [83]
Ag	H_2O	$(CH_3)_4N^+$, Cl^-, Br^-, I^-	Decomposition	[42]
Li	THF, 2Me-THF	PTHF, thin film	Decomposition	[83], [84], [85], [86]
Fe (C)	H_2O/Na_2CO_3–$NaHCO_3$	$FeCO_3$, Fe_3O_4, FeOOH, $Fe(OH)_2$	Corrosion products	[5]
Ag	H_2O	pz, pzH^+, DHPz	Orientation, decomposition	[34], [35]

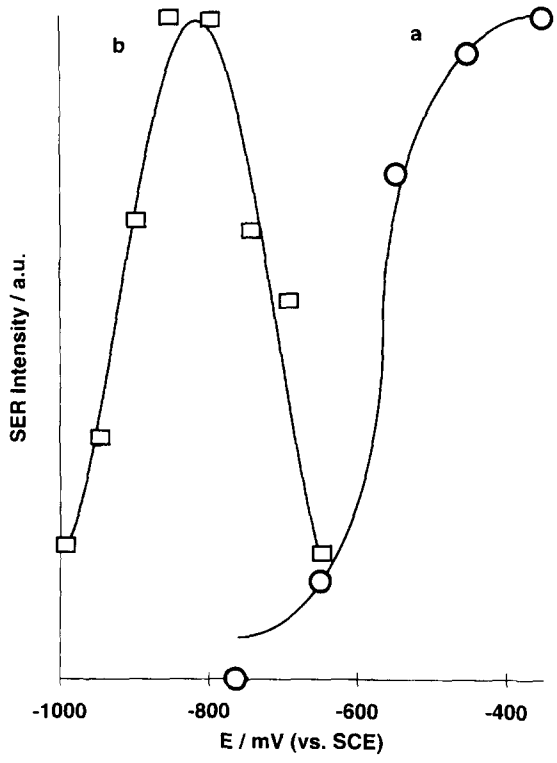

Fig. 5. Potential profiles of (a) 1,4-dyhydropyrazinium cation and (b) pyrazine adsorbed onto a silver electrode from 1.0 M Br^- solution [35]. $\lambda_{exc.} = 514.5$ nm.

coordinates which are relaxed by the electronic excited state.

4. SERS experimental results and discussion

Some of the common features of SERS will be illustrated by data obtained in our laboratory. A summary of the electrochemical systems studied in our laboratory is presented in Table 2. The objective is to present to a non-SERS specialist the expected response of the enhanced Raman intensities to applied potential, excitation energy, and surface coverage changes. Some direct applications of the technique — to determine molecular orientation and to study electrochemical reactions — will be discussed as examples.

4.1. Potential dependence of the SERS intensities

Fig. 5 shows SER intensities vs. applied potential for pyrazine (pz) [34] and the 1,4-dihydropyrazine (DHPz) [35] cation. These plots are known as potential profiles. A bell shaped curve for the neutral molecule and a decrease in the SER intensity as the potential becomes negative for the cation are observed. The enhancement of the local electric

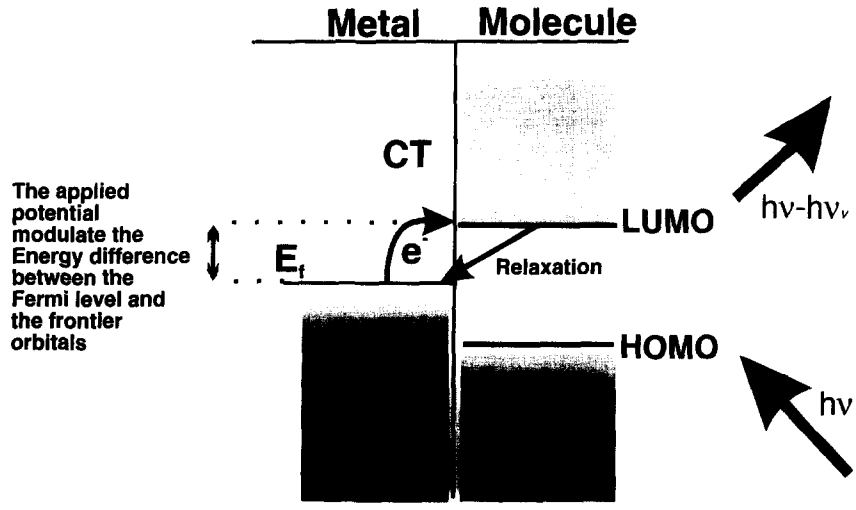

Fig. 6. For adsorbed molecules containing empty low energy π^* orbitals, an electron is transferred from the metal's Fermi level to the LUMO. This process is in resonance with the energy of the incident photon ($h\nu$). The energy of the Fermi level can be modulated by the applied potential; the energy of the Fermi level either increases or decreases as a negative or positive potential, respectively, is applied.

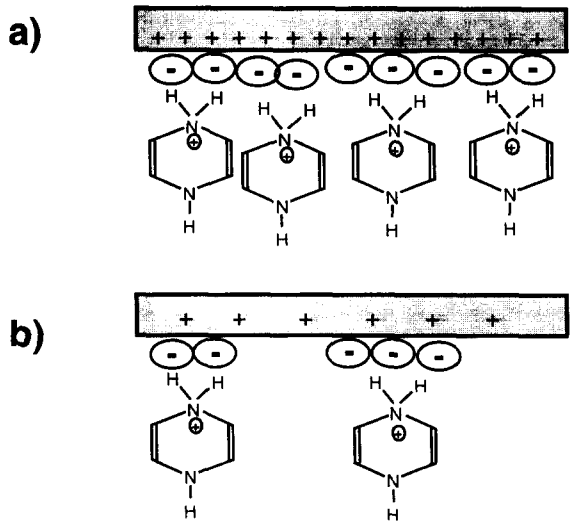

Fig. 7. The coadsorption of a cation and a halide onto the metallic surface. (a) At potentials more positive than the point of zero charge (pzc), the halide is specifically adsorbed onto the electrode surface. (b) As a more negative potential is applied, the amount of adsorbed halide decreases, and the cation also leaves the surface [35].

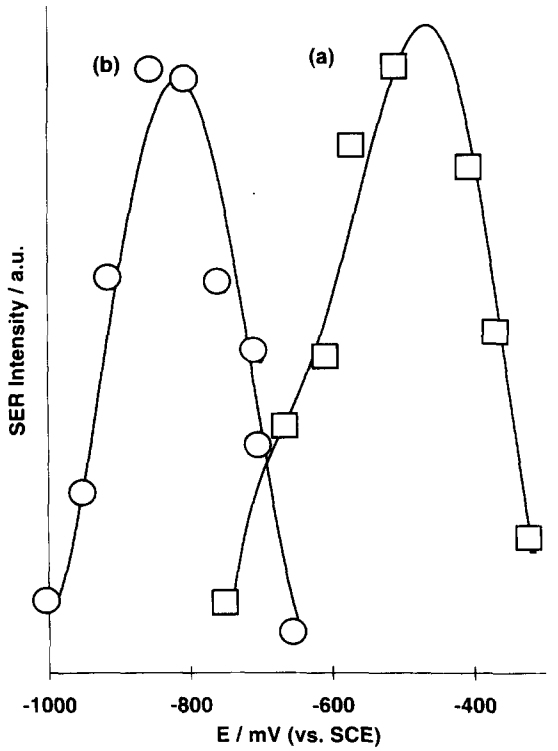

Fig. 8. Potential profiles of pyrazine adsorbed onto a silver electrode. The electrode was activated in the presence of pyrazine. (a) 1.0 M KCl + 0.01 M pyrazine. (b) 1.0 M KBr + 0.01 M pyrazine.

field depends only on the metal characteristics; hence, under the EM model, the change in the SER intensity with potential largely reflects a change in the surface coverage. In fact, the surface coverage of a neutral molecule rises to a maximum near the point-of-zero-charge (pzc) and then falls off as the electrode potential is swept through a suitable range [36]. Under the CT model, the maximum could result when the potential change moves the Fermi level in and out of the resonance condition [37,38]. This situation is illustrated by Fig. 6.

The DHPz cation cannot interact directly with the positive electrode surface; rather, the cations bind to a halide layer, as illustrated in Fig. 7, evident from low frequency SERS bands [34]. As the potential is made less positive, the halide leaves the surface, and the coadsorbed cation concentration also decreases. This ion-pair model has been invoked for the adsorption of pyridinium cations [39], diprotonated 1,4-diazabicyclo[2.2.2]octane (DABCO) [40], and solvated lithium cations [41] onto halide-coated silver. It is interesting to note that the bulky tetramethylammonium cation, with its buried charge, has a maximum intensity near the pzc, thus behaving as an uncharged species [41,42]. The enhancement at a distance (the halide layer is the spacer) is consistent with the EM mechanism.

The potential at which the SER intensity maximizes (E_{max}) is also dependent on the nature and concentration of the supporting electrolyte. For instance, Fig. 8 shows potential profiles for pyrazine adsorbed onto silver electrodes covered with two different halides — chloride and bromide. The specific anion adsorption shifts the pzc of the electrode to negative values. The overall effect is a shift in E_{max} to negative values as the amount of adsorbed anion increases on the electrode surface. Bromide is more strongly adsorbed onto the surface than chloride; therefore, the E_{max} obtained for bromide medium is expected to be shifted to more negative potentials when compared to chlorides, as borne out by Fig. 8. The same argument can be used to account for the changes at different electrolyte concentrations. A more concentrated solution of the same halide yields a more negative E_{max}.

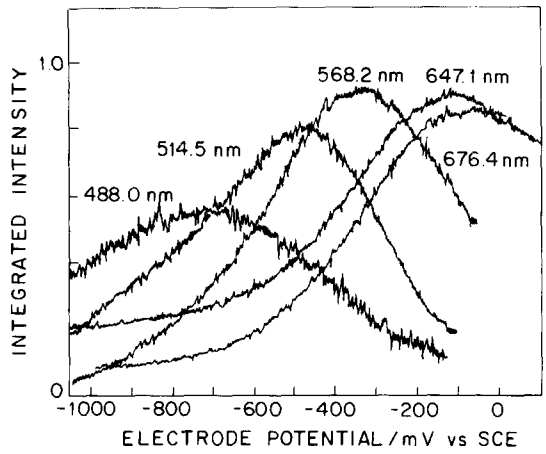

Fig. 9. SERS potential profiles of DABCO adsorbed onto a silver electrode in 0.1 M perchlorate supporting electrolyte. The excitation wavelengths are indicated (from Ref. [44]).

4.2. Dependence of the SERS intensities on excitation energy

The EM contribution to the enhancement depends on the dielectric constant of the metal, and the dielectric constant is dependent on the incident light. Therefore, different relative enhancements are expected for different metals at different excitation wavelengths. For instance, the relative enhancements for silver peaks at about 700 nm, and the relative enhancement for copper and gold increase monotonically as the wavelength increases [43]. The enhancement expected from the EM model depends only on metallic properties; hence, vibrational modes of similar symmetry species should be enhanced by the same amount at a given potential (respecting the selection rules). Therefore, the potential at which the SER intensities reach a maximum (E_{max}) is expected to be the same for similar modes of vibration, and is not expected to change for different incident wavelengths.

Fig. 9 shows the potential profiles for DABCO adsorbed onto a silver surface, measured with different exciting wavelengths [44]. It can be seen that E_{max} shifts to more negative potentials as the photon excitation energy increases. This behavior can be interpreted in terms of the CT argument illustrated in Fig. 6. The potentials at which resonance is satisfied are different for different excitation energies. Fig. 10 shows the dependence of E_{max} on excitation energy for DABCO adsorbed onto silver electrodes in the presence of different electrolytes. The linear relationship of E_{max} vs. photon energy plots is expected from the CT model [45]. In fact, the sign of the slope of these plots reveals the direction of the CT process. A positive slope indicates a CT process from the metal's Fermi level to the LUMO orbital of the molecule. This kind of result is expected for molecules contain-

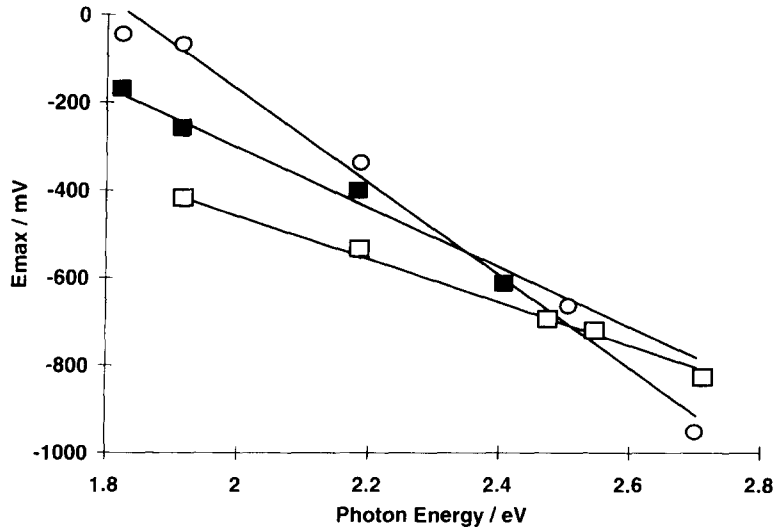

Fig. 10. Plot of the potentials of the maximum intensity of the potential profiles of the ν_4 DABCO band vs. the excitation photon energy for three supporting electrolytes: (○) 0.1 M $KClO_4$; (■) 0.1 M KF; (□) 0.1 M KCl (from Ref. [44]).

ing a low-lying π^* orbital, such as pyridine and pyrazine. A negative slope indicates a CT process from the HOMO molecular orbital to the Fermi level [12]. Situations can arise where several CT processes occur for the same species adsorbed onto an electrode [46]. The dependence of E_{max} on excitation wavelength has been used to indicate a quantitative contribution of the CT mechanism to the overall effect [47]. However, care must be taken because the shift in E_{max} depends on the concentration of the specifically adsorbed halide. For instance, for pyrazine adsorbed onto a silver electrode from a 1.0 M bromide solution, there was no observable shift of E_{max} with excitation energy [34]; however, a CT contribution to the SERS of pyrazine has been suggested [45] for less concentrated halide solutions.

4.3. Dependence of the SERS intensities on surface roughness

SERS intensities depend dramatically on the surface morphology. An AFM picture of a typical SERS-active electrode is presented in Fig. 11. Studies involving the dependence of the SERS intensities on the surface morphology, measured by SEM, have been performed [48,49] for pyridine and chloride adsorbed onto polycrystalline silver electrodes. It was found that the SERS intensities increased as the diameter of the surface features decreased and the two-dimensional density of roughness features increased. The SERS intensities reached a maximum when the average diameter of the surface bumps was between 90 and 100 nm. These results are in good agreement with a recent study of the dependence of the SER signal on the parameters of the ORCs [50]; a r.m.s. roughness of 80 nm for an optimal signal was reported. The importance of these small-scale bumps for optimal SERS intensities was suggested from an STM study of the changes in Ag(111) surface morphology after an electrochemical roughening procedure [51]. The relationship between surface roughness, determined experimentally, and SERS intensity is in agreement with the predictions of the EM mechanism.

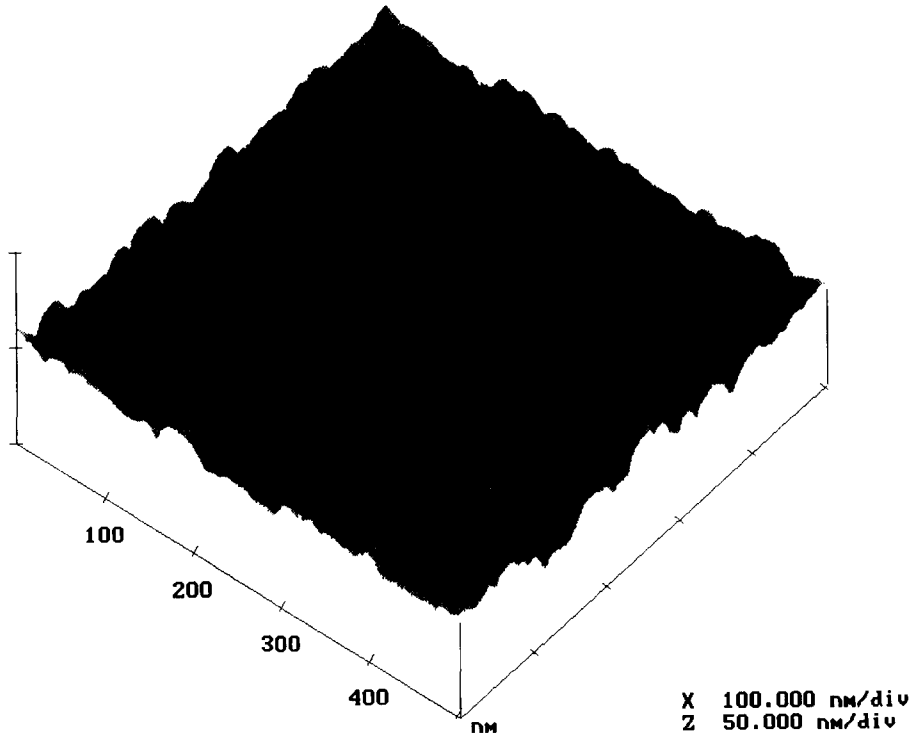

Fig. 11. AFM image of an activated gold electrode. The activation procedure is described elsewhere [23]. Seven ORCs were performed.

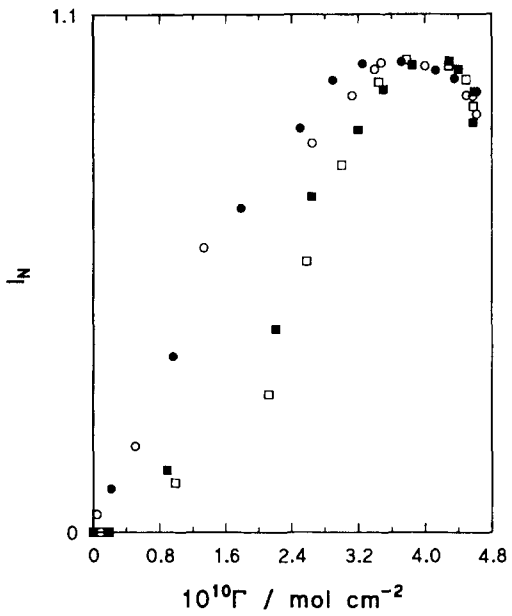

Fig. 12. Plot illustrating the relationship between normalized SER intensity (I_N) and surface coverage (Γ) for different pyridine concentrations: (○) 3×10^{-3} M; (●) 10^{-3} M; (□) 10^{-4} M; (■) 4×10^{-5} M. (from Ref. [55]).

4.4. Dependence of the SERS intensities on surface coverage

Knowledge of the dependence of SERS intensity on surface coverage is very important for the application of SERS to electrochemical problems. SERS intensities must be compared with surface coverage data obtained from independent electrochemical measurements. Electrochemical surface coverage data are not always available for the commonly studied SERS systems, but such information is being produced in our Centre [52]. The relationship between the electrochemical SERS intensity and surface concentration has been investigated for halides and pseudohalides adsorbed onto silver electrodes [53,54]. Fig. 12 shows a plot of normalized SERS intensity vs. surface coverage, obtained by chronocoulometry, for pyridine adsorbed onto a "smooth" gold electrode [55]. An almost linear relationship was found for surface concentration values up to 2/3 of a monolayer. The decrease in SERS intensity at high surface coverage values was attributed to depolarization effects on the local electric field [56].

4.5. Determination of the molecular orientation using SERS

In Fig. 13 the spectrum of pyrazine adsorbed onto a silver electrode is compared with that of the aqueous solution pyrazine species [34]. Noting the representation of the vibrational modes, given in Fig. 14, it can be concluded that the vibrations with components along the N–N axis are most enhanced. For instance, in contrast with aqueous pyrazine, this spectral region is dominated by the 630 cm^{-1} band (Fig. 13c) rather than the $\approx$ 697 cm^{-1} band (Fig. 13a and Fig. 13b). This result suggests that pyrazine is adsorbed end-on

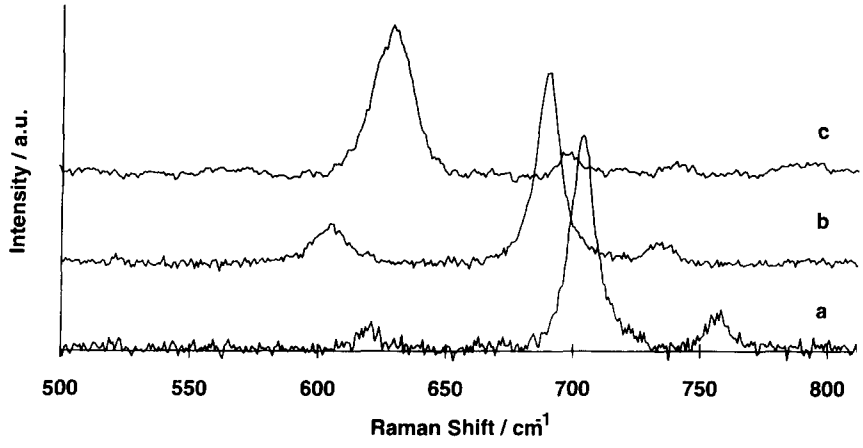

Fig. 13. The 500–800 cm^{-1} region of the Raman spectrum of (a) 1.0 M aqueous pyrazine solution and (b) 1.0 M aqueous pyrazine in 3.0 M HCl solution. The spectral features are due to the monoprotonated pyrazine cation, pzH^+. (c) SER spectrum of pyrazine on a silver electrode from 1.0 M KBr + 0.1 M pyrazine solution. E = – 600 mV. The electrode was activated in the absence of pyrazine [34].

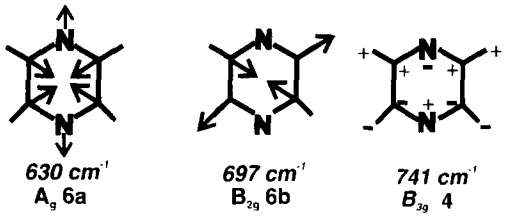

Fig. 14. Schematic representation of three pyrazine vibrational modes. The Wilson numbering scheme is presented for each representation together with the SER vibrational frequency, in cm^{-1}.

(attached by the N lone pair) to the electrode surface. However, it is very important to point out that such a conclusion cannot be drawn based just on one band; all allowed bands in the SER spectrum must be considered. In the particular case of pyrazine, the end-on adsorption was confirmed by a preferential enhancement of the modes containing the α_{ZZ} term of the molecular polarizability, followed by those with α_{ZY} and α_{XZ} components; the modes containing the α_{XY} components presented the weakest features [34]. Bands forbidden in the NRS also appear in the adsorbed pyrazine spectrum. These bands are activated by a field gradient mechanism [57]. Another procedure, which has limited application, is to compare the intensities of a symmetric and antisymmetric mode of the species from a SERS experiment and NRS; a marked change (a reversal) of intensity during a potential sweep can signal an orientation change [58,59].

4.6. Using SERS to identify products of electrochemical decomposition

The SERS technique has considerable potential for the study of Faradaic electrochemical processes. Electrochemical reaction products of organic [60,61,35] and inorganic compounds can often be identified. Fig. 15 shows the vibrational bands from carbon monoxide on a copper electrode [62]. The CO, formed from CO_2 reduction in bicarbonate medium, is an intermediate in the reduction process. Several bands assignable to an adsorbed CO species are observed. The high frequency bands are due to a C–O stretch mode. The low frequency bands are due to the metal–carbon stretching and the frustrated rotational modes, which are described elsewhere [62].

4.7. Hazards of the application of SERS to electrochemical problems

The necessity of a rough surface, the limited number of metals, and the non-linear relationship between SERS intensity and surface concentration for all applied potentials are the most obvious problems

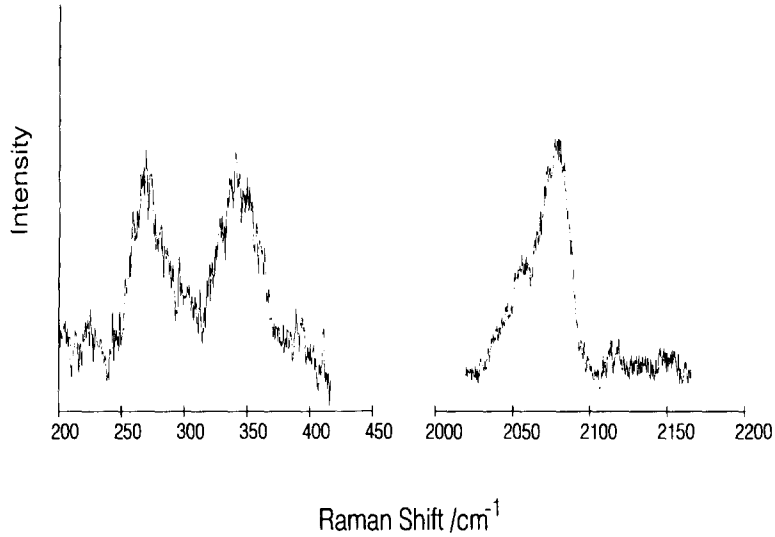

Fig. 15. The SERS spectrum of the metal–carbon and carbon–oxygen modes of CO adsorbed onto a copper electrode ($E = -1.5$ V (vs. SCE)) [62].

restricting the application of SERS to electrochemical systems. However, there are other experimental pitfalls of which the non-SERS specialist should be aware. One of them concerns the activation procedure. The ORCs can either be performed with a solution containing the adsorbent species or the adsorbent can be added to the solution after the electrode has been activated. The former procedure gives a better signal-to-noise ratio; however, it has been shown that this procedure can trap the adsorbent or one of its electrochemical reaction products on the metallic surface [63–65]. Therefore, the spectrum obtained after activation in the presence of the adsorbate must always be compared to a spectrum obtained in the absence of the adsorbate to avoid misassignments and false conclusions [35].

Another problem is the time dependence of the SER signal. This time dependence has been attributed to the thermally-induced desorption of the adsorbed species, followed by the incorporation of the "free" SERS-active sites into the metal lattice [66]. This hypothesis was supported by an in situ STM study of the morphology changes of silver electrodes following an ORC in halide medium [67]. The roughness features were found to relax quickly, and the electrode surface became more "flat" with time. The problem of the time evolution of the SER signal can be minimized by performing a "shallow" ORC prior to each measurement [55].

The SERS-active sites can also be quenched by a potential sweep to very negative values. In this case, the desorption of the adsorbate is induced by the applied potential [68]. Oxidation of the active sites, mainly the adatoms, by molecular oxygen can also quench SERS intensity [69]. The stability of the SERS-active sites is found to be higher for gold than for copper and silver electrodes.

The silver electrode suffers from a problematic form of carbonaceous contamination. The most likely source is atmospheric CO_2 which apparently reaches the electrode surface and decomposes [70]. The spectrum of this material consists of a series of broad bands at about 1350 and 1600 cm^{-1}, attributed to graphitic carbon vibrations [71], and a series of bands, possibly attributable to CH stretching modes between 2700 and 2950 cm^{-1}; these bands are evident in many SERS measurements. In many cases (e.g. pyridine, pyrazine and other strong scatterers) they have no great impact since the SERS of these molecules is intense and contamination bands do not appear in the spectral region of interest. The major problem with this contamination occurs when its presence obscures the spectral region of other compounds that one may wish to examine. This problem does not occur for either copper or gold electrodes and is, therefore, not a characteristic of the SERS process; it seems to be inherent to silver electrodes, and is thus attributed to the unique surface chemistry of silver.

5. Summary

A design for a spectroelectrochemical cell for SERS has been described. Procedures for activating the surface of silver, copper and gold electrodes have been presented. Although activation in the presence of the molecule of interest leads to a greater SERS intensity, there is a possibility that spurious Raman bands from entrapped decomposition products can lead to erroneous conclusions. The mechanisms and selection rules for SERS have been reviewed. Experimental results that confirm both the EM mechanism and the CT mechanism have been presented. The dependence of SERS intensity on electrode potential, excitation energy, surface roughness, surface coverage and some pitfalls to be avoided when conducting SERS experiments were described. Examples of the application of SERS to the determination of molecular orientation and to the identification of electrochemically-generated products were discussed.

Acknowledgements

This work was supported by grants from the Natural Sciences and Engineering Research Council of Canada.

References

[1] D.L. Jeanmaire and R.P. Van Duyne, J. Electroanal. Chem., 84 (1977) 1.
[2] M.G. Albrecht and J.A. Creighton, J. Am. Chem. Soc., 99 (1977) 5215.

[3] H. Seki, J. Electron Spectrosc. Relat. Phenom., 39 (1986) 289.
[4] J. Gui and T. Devine, Corros. Sci., 36 (1994) 441.
[5] M. Odziemkowski, J. Flis and D.E. Irish, Electrochim. Acta, 39 (1994) 2225.
[6] Y. Misono, M. Nagase and K. Itoh, Spectrochim. Acta, 50A (1994) 1539.
[7] N. Matsuda, T. Sawaguchi, M. Osawa and I. Uchida, Chem. Lett., (1995) 145.
[8] I. Nabiev, I. Chourpa and M. Manfait, J. Raman Spectrosc., 25 (1994) 13.
[9] V.J.P. Gouveia, I.G. Gutz and J.C. Rubin, J. Electroanal. Chem., 371 (1994) 37.
[10] C. Rodger, W.E. Smith, G. Dent and M. Edmondson, J. Chem. Soc., Dalton Trans., (1996) 791.
[11] R.K. Chang and B.L. Laube, CRC Crit. Rev. Solid State Mater. Sci., 12 (1984) 1.
[12] R.L. Birke and J.R. Lombardi, in R.J. Gale (Ed.), Spectroelectrochemistry — Theory and Practice, Plenum, New York, 1988, Chapter 6, p. 263.
[13] R.K. Chang, in C. Gutierrez and C. Melendres (Eds.), Spectroscopic and Diffraction Techniques in Interfacial Electrochemistry — NATO ASI Series, Series C, no. 320, Kluwer, Boston, MA, 1990, p.155.
[14] R.L. Birke, T. Lu and J.R. Lombardi, in R. Varma and J.R. Selman (Eds.), Techniques for Characterization of Electrodes and Electrochemical Processes, Wiley, New York, 1991, Chapter 5, p. 211.
[15] E.S. Brandt and T.M. Cotton, in B.W. Rossiter and R.C. Baetzold (Eds.), Physical Methods of Chemistry Volume IXB — Investigations of Surfaces and Interfaces — Part B, 2nd edn., Wiley, New York, 1993, Chapter 8, p. 633.
[16] W. Suetaka, Methods of Surface Characterization — Surface Infrared and Raman Spectroscopy: Methods and Applications, Plenum, New York, 1995.
[17] J.E. Pemberton, in H.D. Abruna (Ed.), Electrochemical Interfaces: Modern Techniques for in situ Interface Characterization, VCH, New York, 1991, Chapter 5, p. 193.
[18] B. Pettinger, in J. Lipkowski and P.N. Ross (Eds.), Adsorption of Molecules at Metal Electrodes, VCH, New York, 1992, Chapter 6, p. 285.
[19] T.M. Cotton, in R.J.H. Clark and R.E. Hester (Eds.), Spectroscopy of Surfaces — Advances in Spectroscopy, Vol. 16, Wiley, New York, 1988, Chapter 3, p. 91.
[20] R.L. Garrell, Anal. Chem., 61 (1989) 401A.
[21] S.H. Macomber, T.E. Furtak and T.M. Devine, Chem. Phys. Lett., 90 (1982) 439.
[22] H. Furukawa, M. Takahashi and M. Ito, J. Electroanal. Chem., 256 (1988) 213.
[23] P. Gao, D. Gosztola, L.-W.H. Leung and M. Weaver, J. Electroanal. Chem., 233 (1987) 211.
[24] A. Campion, in J.T. Yates and T.E. Madey (Eds.), Vibrational Spectroscopy of Molecules on Surfaces, Plenum, New York, 1987, Chapter 8, p. 345.
[25] U. Wenning, B. Pettinger and H. Wetzel, Chem. Phys. Lett., 70 (1980) 49.
[26] T.T. Chen, J.F. Owen, R.K. Chang and B.L. Laube, Chem. Phys. Lett., 89 (1982) 356.
[27] A. Otto, I. Mrozek, H. Grabhorn and W. Akemann, J. Phys. Condens. Matter, 4 (1992) 1143.
[28] A. Otto, J. Raman Spectrosc., 22 (1991) 743.
[29] M. Moskovits, Rev. Mod. Phys., 57 (1985) 783.
[30] E.J. Zeman and G.C. Schatz, J. Phys. Chem., 91 (1987) 634.
[31] R.J.H. Clark and T.J. Dines, Angew. Chem. Int. Ed. Engl., 25 (1986) 131.
[32] J.A. Creighton, in R.J.H. Clark and R.E. Hester (Eds.), Spectroscopy of Surfaces — Advances in Spectroscopy, Vol. 16, Wiley, New York, 1988, Chapter 2, p. 37.
[33] H. Grabhorn and A. Otto, Vacuum, 41 (1990) 473.
[34] A.G. Brolo and D.E. Irish, J. Electroanal. Chem., 414 (1996) 183.
[35] A.G. Brolo and D.E. Irish, J. Chem. Soc., Faraday Trans., 93 (1997) 419.
[36] R. Guidelli, in J. Lipkowski and P.N. Ross (Eds.), Adsorption of Molecules at Metal Electrodes, VCH, New York, Chapter 1, 1992, p. 1.
[37] J.R. Lombardi, R.L. Birke, T. Lu and J. Xu, J. Chem. Phys., 84 (1986) 4174.
[38] J.C. Rubin, P. Corio, M.C.C. Ribeiro and M. Matz, J. Phys. Chem., 99 (1995) 15 765.
[39] D.J. Rogers, S.D. Luck, D.E. Irish, D.A. Guzonas and G.F. Atkinson, J. Electroanal. Chem., 167 (1984) 237.
[40] D.A. Guzonas, D.E. Irish and G.F. Atkinson, Langmuir, 5 (1989) 787.
[41] Z. Deng and D.E. Irish, Langmuir, 10 (1994) 586.
[42] Z. Deng and D.E. Irish, J. Phys. Chem., 98 (1994) 11 169.
[43] B. Chase and B. Parkinson, J. Phys. Chem., 95 (1991) 7810.
[44] D.A. Guzonas, D.E. Irish and G.F. Atkinson, Langmuir, 6 (1990) 1102.
[45] J. Thietke, J. Billmann and A. Otto, in B. Pullman, J. Jortner, A. Nitzan and B. Gerber (Eds.), Dynamics on Surfaces, Reidel, Boston, MA, 1984, p. 345.
[46] J.C. Rubin, M.L.A. Temperini, P. Corio, O. Sala, A.H. Jubert, M.E. Chacon-Villalba and P.J. Aymonino, J. Phys. Chem., 99 (1995) 345.
[47] A. Kudelski and J. Bukowska, Chem. Phys. Lett., 222 (1994) 555.
[48] M.A. Bryant and J.E. Pemberton, Langmuir, 6 (1990) 750.
[49] D.D. Tuschel, J.E. Pemberton and J.E. Cook, Langmuir, 2 (1986) 380.
[50] S. Kruszewski, Surf. Interface Anal., 21 (1994) 830.
[51] G. Aloisi, A.M. Furtikov and R. Guidelli, Surf. Sci., 296 (1993) 291.
[52] J. Lipkowski and L. Stolberg, in J. Lipkowski and P.N. Ross (Eds.), Adsorption of Molecules at Metal Electrodes, VCH, New York, 1992, Chapter 4, p. 171.
[53] M.J. Weaver, J.T. Hupp, F. Barz, J.G. Gordon II and M.R. Philpott, J. Electroanal. Chem., 160 (1984) 321.
[54] H. Wetzel, H. Gerischer and B. Pettinger, Chem. Phys. Lett., 78 (1981) 392.
[55] L. Stolberg, J. Lipkowski and D.E. Irish, J. Electroanal. Chem., 300 (1991) 563.
[56] C.A. Murray and S. Bodoff, Phys. Rev. B, 32 (1985) 671.
[57] J.K. Sass, H. Neff, M. Moskovits and S. Holloway, J. Phys. Chem., 85 (1981) 621.

[58] Z. Deng and D.E. Irish, J. Phys. Chem., 98 (1994) 9371.
[59] J.E. Pemberton, M.A. Bryant, R.L. Sobocinski and S.I. Joa, J. Phys. Chem., 96 (1992) 3776.
[60] T.M. Cotton and M. Vavra, Chem. Phys. Lett., 106 (1984) 491.
[61] M. Takahashi, M. Fujita and M. Ito, Surf. Sci., 158 (1985) 307.
[62] B.D. Smith, D.E. Irish, in S.A. Asher and P. Stein (Eds.), Proceedings of the Fifteen International Conference on Raman spectroscopy, Wiley, Chichester, 1996, p. 742.
[63] K.D. Beer, W. Tammer and R.L. Garrell, J. Electroanal. Chem., 258 (1989) 313.
[64] L. Markwort and P.J. Hendra, Spectrochim. Acta Part A, 49 (1993) 837.
[65] H. Saito, J. Raman Spectrosc., 24 (1993) 191.
[66] R.L. Sobocinski and J.E. Pemberton, Langmuir, 4 (1988) 836.
[67] J.-S. Chen, T.M. Devine, D.F. Ogletree and M. Salmeron, Surf. Sci., 258 (1990) 346.
[68] B. Pettinger and L. Moerl, J. Electron Spectrosc. Relat. Phenom., 29 (1983) 383.
[69] S.H. Nicolai and J.C. Rubin, Vib. Spectrosc., 7 (1994) 175.
[70] M.R. Cooney, M.W. Howard and R.P. Cooney, Chem. Phys. Lett., 71 (1980) 59.
[71] Y. Kawashimand and G. Katagiri, Phys. Rev. B, 52 (1995) 10053.
[72] G.F. Atkinson, D.A. Guzonas and D.E. Irish, Chem. Phys. Lett., 75 (1980) 557.
[73] D.A. Guzonas, G.F. Atkinson, D.E. Irish and W.A. Adams, J. Electroanal. Chem., 150 (1983) 457.
[74] D.A. Guzonas, G.F. Atkinson and D.E. Irish, Chem. Phys. Lett., 107 (1984) 193.
[75] D.E. Irish, L. Stolberg and D.W. Shoesmith, Surf. Sci., 158 (1985) 238.
[76] D.E. Irish, I.R. Hill, P. Archambault and G.F. Atkinson, J. Sol. Chem., 14 (1985) 221.
[77] D.E. Irish, D.A. Guzonas and G.F. Atkinson, Surf. Sci., 158 (1985) 314.
[78] I.R. Hill, D.E. Irish and G.F. Atkinson, Langmuir, 2 (1986) 752.
[79] J. Lipkowski, L. Stolberg, S. Morin, D.E. Irish, P. Zelenay, M. Gamboa and A. Wieckowski, J. Electroanal. Chem., 335 (1993) 147.
[80] T. Ozeki and D.E. Irish, J. Electroanal. Chem., 280 (1990) 451.
[81] T. Ozeki and D.E. Irish, J. Phys. Chem., 96 (1992) 1302.
[82] T. Ozeki and D.E. Irish, J. Phys. Chem., 96 (1992) 1306.
[83] D.E. Irish, Z. Deng and M. Odziemkowski, J. Power Sources, 54 (1995) 28.
[84] M. Odziemkowski, M. Krell and D.E. Irish, J. Electrochem. Soc., 139 (1992) 3052.
[85] M. Odziemkowski and D.E. Irish, J. Electrochem. Soc., 139 (1992) 3063.
[86] M. Odziemkowski and D.E. Irish, J. Electrochem. Soc., 140 (1993) 1546.